

***In-vivo study on the stability of the use of gas
absorption spectroscopy as a technology for
assessing sinus cavity size and oxygen gas
concentration***

Author: Sara Mekamy

Year: 2020

Master's Thesis in
Biomedical Engineering

Supervisors: Prof. Tomas Jansson (Department of Biomedical
Engineering LTH), Dr. Sara Bergsten (GPX Medical AB)



Department of Biomedical Engineering at LTH

Abstract

Sinusitis is a common disease caused by a virus or bacteria, with 84% to 91% of cases caused by a viral pathogen. However, physicians prescribe antibiotics for this disease in 85% of all cases. GPX Medical is a company working on the development of a medical device which, by means of absorption spectroscopy, can determine whether the disease is caused by virus or bacteria supporting, thus, the doctors in decision making. The main purpose of this study is to evaluate the stability of the measurements performed by this medical device, by analyzing the maxillary sinuses size and O₂ concentration in different subjects under a longer period. The first step consisted in performing a pilot study to determine the measurement geometries, number of samples and the updating time for the laser by analyzing a 3-D model of the sinuses and the strength of the signal. This was followed by a preclinical study where measurements on sinuses size and O₂ concentration of five healthy volunteers were performed over a period of one-day, one-week and one-month to analyze the intra- and intersubject variability and determine the best measurement geometry. This pilot study revealed an optimal number of samples of 30 and an optimal updating time for the laser of 2s. From the preclinical study it resulted that the best measurement position is the palate-cheekbone geometry (position 1), which was determined by analyzing the signal strength. The results of the preclinical study show a certain stability of the measurements with low intrasubject variability in most cases, accompanied by differences between the right and the left side, and a higher intersubject variability. However, for better results a newer fiber should be used in the measurements for position 1 and 2.

Acknowledgments

This project started in November 2019 and was pursued at GPX Medical. The aim of this project was to analyze the stability of the measurements on the sinuses, performed by the device for gas absorption spectroscopy developed by GPX Medical, over certain intervals of time. Furthermore, it was of interest to analyze differences between right and left sinus in the same subject, the oxygen content and the intersubject variations.

I would like to thank Sara Bergsten and Dennis Leander, who work at GPX Medical, for their help and support in this project. They were always ready to intervene if something did not work as expected and help in case of doubt about the instrument. They were also available whenever I needed to discuss something with them. My supervisor, Tomas Jansson, also played an important role in this thesis by giving me feedback and helping me improve my work.

Table of Contents

1 Introduction	6
1.1 Scope	9
1.2 Disposition.....	9
2 Background	11
2.1 Sinuses.....	11
2.1.1 Sinusitis.....	12
2.2 Optical spectroscopy	13
2.2.1 Interaction between light and gas	13
2.3 Gas in Scattering Media Absorption Spectroscopy (GASMAS) technology	15
2.3.1 GASMAS biological applications	16
3 Method	20
3.1 Technical instruments.....	20
3.2 Pilot Study	22
3.3 Preclinical Study.....	24
4 Results and discussion.....	25
4.1 Pilot Study	25
4.2 Preclinical Study.....	30
4.2.1 O ₂ and H ₂ O transmission and absorption signals for the different measurement positions.....	31
4.2.2 Absorption path length (APL)	34
4.2.3 Oxygen concentration	40
4.2.4 Challenges.....	43
5 Conclusions	46
6 Bibliography.....	48

1 Introduction

Sinusitis is a common disease which consists in the inflammation of the paranasal sinuses. This can be caused by a virus or bacteria, however, in 84% to 91% of cases the infection is of viral origin (Rosenfeld 2016). Doctors prescribe antibiotics for the treatment of sinusitis in most cases (85% of cases), without knowing if the disease was caused by viruses or bacteria and, since viruses are not affected by antibiotics, the result is an over-prescription of this medication (Rosenfeld 2016). These prescriptions count for 21% of all antibiotics prescribed in the Nordics (Jørgensen et al. 2013) and result in increasingly resistant bacteria and ineffectiveness of antibiotics in the long run, which in turn causes an increase in the number of infection-related deaths (see figure 1).

The techniques that are currently used for sinus infection diagnosis include computerized tomography (CT) and magnetic resonance imaging (MRI). CT is of particular interest for the diagnosis of sinusitis because of its property to display soft tissues, bones and air, allowing to detect abnormal changes in the anatomy of the paranasal sinus cavities (Zinreich et al. 1987). MRI, on the other hand, has the ability to characterize tissues allowing the identification of inflamed and/or abnormal tissues, such as tumors; it can also differentiate between obstructive secretion and soft tissues, which is important when investigating sinuses (Raut and Jankharia 2009). However,

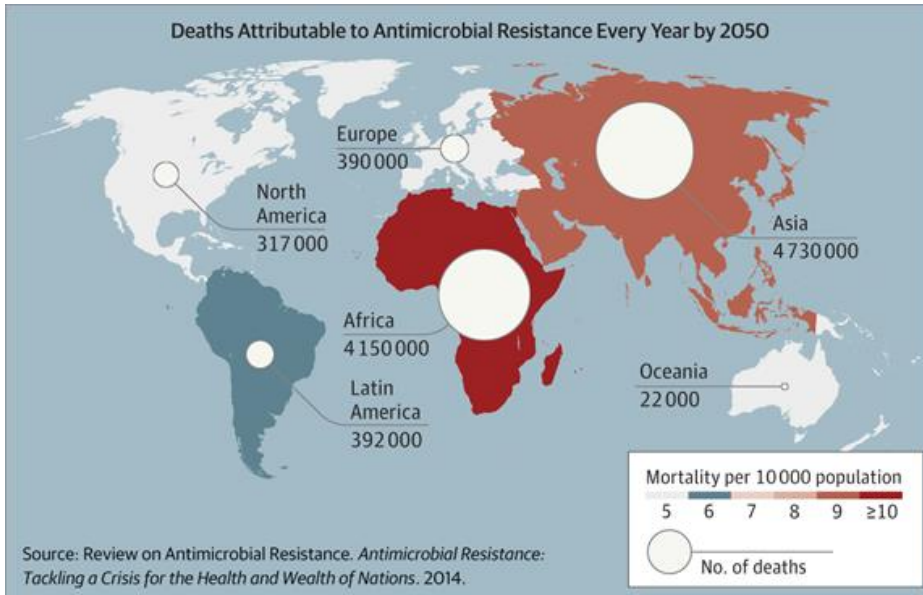


Fig. 1 Deaths due to increasing bacterial resistance to antibiotics by 2050.

these techniques have some drawbacks that make them difficult to use for routine evaluations of the paranasal sinuses. These drawbacks include high cost for both techniques, patient exposure to radiation for CT and disadvantages, such as claustrophobia and incompatibility of pacemakers with the technique, for MRI (Raut and Jankharia 2009; Fatterpekar et al. 2008). Additionally, the time required when using these methods is also longer as patients must be included in a queue system and admitted to other facilities for the investigation. Therefore, there is a need to develop a method that is more safe, cost effective, readily available and simple to use, to assist doctors in the investigation of the sinuses and improve the ability for correct diagnosis, and, most important, reduce the prescription of antibiotics.

Gas in Scattering Media Absorption Spectroscopy (GASMAS) is a technique used to investigate free gas inside pores or cavities surrounded by a highly light scattering media. GASMAS technology is based on Tunable Diode Laser Absorption Spectroscopy (TDLAS), which uses the interaction (absorption and emission) between light and gas molecules to determine the concentration of a certain component in a gas stream (Larsson et al. 2019).

This technology has also been used in studies to investigate gas-filled cavities in the human body, including lungs and sinuses (Larsson et al. 2019; Huang et al. 2015). The main goal was to measure the oxygen concentration in these cavities for medical assessments in a non-intrusive way, (Huang et al. 2015).

GPX Medical is a company in Lund, that is working with the development of a medical device which, by means of laser gas absorption spectroscopy, can measure oxygen gas concentration within the maxillary sinuses and obtain an estimation of the free gas volume in the cavities. These parameters might correlate to whether a sinus infection is caused by viral or bacterial pathogens. This can be determined by measuring oxygen content in the maxillary sinuses using the GASMAS method. The company's hypothesis is that if the disease is caused by certain bacteria, the oxygen content of the sinuses should be less due to the fact that some bacteria consumes oxygen. Now, GPX medical wants to gather information about the stability of the measurements that are obtained through their instrument. The needed information will be collected through this study, which will measure the variation of the O₂ concentration in the sinuses and their size in five volunteers, for a month, under different intervals of time.

Previous studies have already investigated the stability of the GASMAS signals from the sinuses (Huang et al. 2015; Persson et al. 2007). However, these studies were designed in a different way compared to this one. One of these studies is the one carried out by Huang J. et al. (2015), where he and his team investigated the GASMAS signals from four healthy volunteers under a period of six consecutive days (Huang et al. 2015). In the mentioned study, the evaluated instrument had a different configuration and set-up compared to the instrument used in this study and the cavities under analysis were the frontal sinuses. Furthermore, the volunteers were only followed under a period of six days. Another study made by Persson L. et al (2007) examined GASMAS signals obtained from different probe positions in 11 volunteers, however no follow-up for measurements stability was done over a longer period of time (Persson et al. 2007).

1.1 Scope

The aim of the thesis is to investigate the stability of the measurements performed with the medical device developed by GPX Medical AB. This is carried out by measuring oxygen gas concentration within and measuring the free gas volume of the maxillary sinuses of healthy volunteers at different times and intervals.

In more detail, the goal is to:

- Gain a deeper understanding of GASMAS technology and participate in probe development at GPX Medical
- Design and conduct a study that measures sinus sizes and the oxygen gas concentrations. Variables to explore are:
 - Probe positions
 - Laser parameters and exposure time
 - Left / right sinus comparison
 - Comparison of the measurement from the same person for one-day, five consecutive days and variations over a month
 - Comparison of the measurement from different subject
- Develop clinical protocol for scientific studies
- Evaluate data and answer the questions of stability on the sinus measurements

1.2 Disposition

This paper is organized into four main sections. The first section is the introduction which contains the information necessary to understand the rest of the work and its purpose. The second section contains the background which gives an overview about the sinuses, laser spectroscopy and GASMAS technology. The third section consists of the method, where the technical instruments, used in the study, are introduced, followed by the

method used in the pilot study and the successive preclinical study. In the fourth section the results obtained from the study are presented in different subsections and discussed. The challenges encountered during this project are also described here. Finally, in the last part the conclusions are presented.

2 Background

2.1 Sinuses

The paranasal sinuses are connected, air-filled cavities located in the skull. There are four sets of paired sinuses known as: sphenoid, ethmoid, maxillary and frontal (see figure 2). These are divided into two groups based on their drainage pathway. The first group, which drains into the middle meatus,

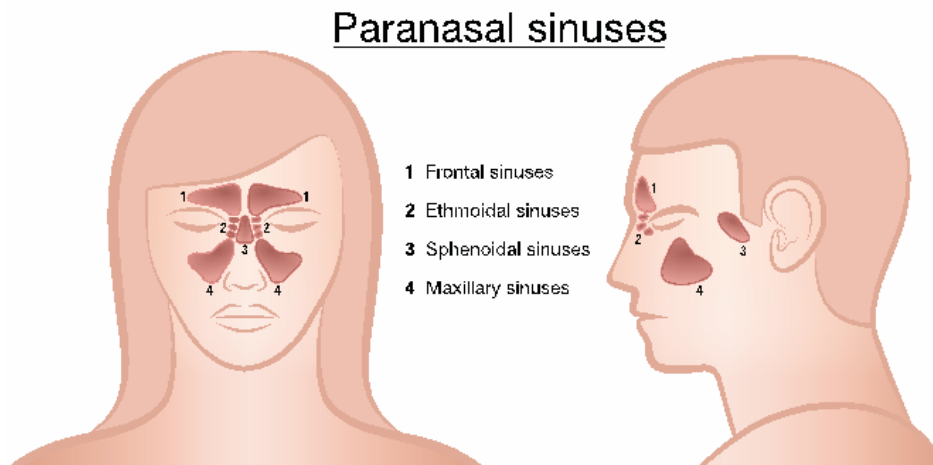


Fig. 2 Paranasal sinuses

includes the maxillary, frontal and anterior ethmoid sinuses (the anterior sinuses group). The second group instead drains into the sphenoethmoidal

recess and includes the posterior ethmoid and sphenoid sinuses (the posterior sinuses group) (Alsaied 2017). The maxillary sinus is the largest air-filled sinus in the body.

There are different hypotheses about the function of the sinuses and some of these include lightening the skull, amplifying the sound and the voice, increasing the perception of odors, keeping the inside of the nose moisturized and draining of course (Jankowski et al. 2016). Among the functions of the sinuses, there is also the generation of nitric oxide (NO), which production is regulated by nasal breathing, through the monitoring of its presence in the exhaled air. This gas, which is inhaled at every breath, increases the intake of oxygen through local vasodilation (of the pulmonary vessels) for better lung ventilation. In Addition, this gas provides protection against viral and bacterial infections in the airways. Another role of NO consists in warming and humidifying inhaled air (Jankowski et al. 2016).

2.1.1 Sinusitis

In healthy sinuses the mucus, which is produced by the ciliated columnar epithelium, is transported by the cilia to the sinus ostia where is drained into the nasal space (Morcom et al. 2016). In case of disease, the transport system becomes impaired because of a reduced ciliary activity or obstruction. In these conditions, swelling and blockage of the sinuses, caused by environmental or host factors, creates ideal conditions for infectious agents to grow leading to sinusitis (Morcom et al. 2016). Sinusitis is a very common condition, defined as the inflammation of the paranasal sinuses (Morcom et al. 2016). Sinusitis presents itself in a wide spectrum and it is classified according to its duration: acute sinusitis which lasts up to one-month, subacute sinusitis lasts one to three months and chronic sinusitis which lasts more than three months (Rosenfeld 2016). Acute sinusitis is normally caused by a bacterial or viral infection. Among the symptoms of acute sinusitis, in adults, there are purulent nasal discharge, nasal obstruction, facial pain, pressure and headaches (Rosenfeld 2016). Viral infection accounts for 90% of the cases of acute sinusitis, while only 0.5%

to 2% of the cases develop into a bacterial infection. Despite this fact, antibiotics are prescribed for more than 85% of the patients with acute sinusitis (Rosenfeld 2016).

2.2 Optical spectroscopy

Optical spectroscopy is the study of the emission and absorption of electromagnetic radiation by matter. It offers an efficient way to characterize samples and it gives information about their chemical composition. This interaction between light and matter depends on the type of molecule and its surroundings, and it also gives information about parameters such as concentration, temperature, pressure, etc. Solids and liquids interact with light in a different way from gases. This is because their molecules are interconnected and they affect each other causing light to be absorbed in a broader spectrum, compared to the case where atoms/molecules are free.

The following section will give an insight into how light interacts with gases.

2.2.1 Interaction between light and gas

Light and atoms/molecules, interact through absorption and emission of photons. The absorption and emission of light by an atom or a molecule occurs when there is a transition between two energy states. This transition can only take place when the amount of energy absorbed or emitted by an atom or a molecule is equal to the difference between the two energy states (Parson 2015). Electrons vibrate at a specific frequency, which is known as their 'natural frequency'. Absorption takes place when light of the same frequency of the electron hits the atom/molecule causing the electron to become excited and the atom to transit from a lower to a higher energy state. Light emission by a atom/molecule, instead, occurs when an atom/molecule transits from a higher energy state to a lower one, emitting a photon with an

amount of energy equal to the difference between the two energy states (Parson 2015).

Spectral lines are dark (absorption lines) or bright lines (emission lines) that form in an otherwise continuous spectrum as a result of light absorption or emission by a molecule or atom (see Figure 3). As mentioned above gases interact with light in a different way from solids and liquids. This is because the transition between two energy states in the free molecule of a gas is quantized and this leads to the creation of narrow spectral lines, compared to the case of solid and liquids where light absorption and emission gives rise to a broader spectrum (Lewander 2010).

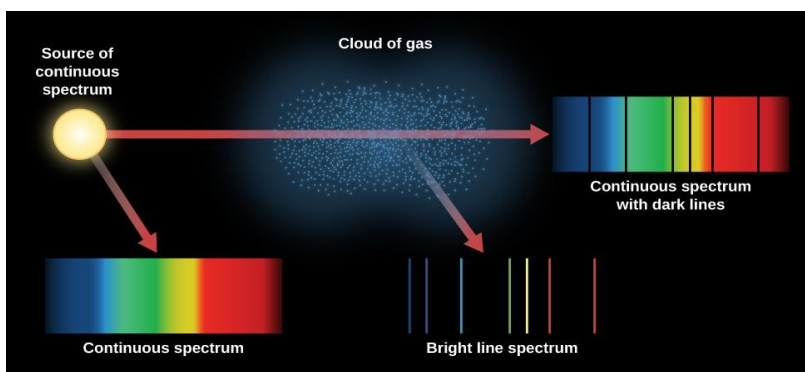


Fig. 3 Absorption and emission lines of a cloud of gas hit by a continuous source of radiation (image brought from: Astronomy. Provided by: OpenStax CNX. Locate at:

<http://cnx.org/contents/2e737be8-ea65-48c3-aa0a-9f35b4c6a966@10.1>).

The most common technique for quantitative gas analysis is called Tunable Diode Laser Spectroscopy (TDLAS). TDLAS uses a frequency-tuned diode laser to scan over one of the absorption lines of the gas under examination. In order to get an absorption signal, the wavelength of the laser is modulated, by changing the intensity of the injected current, so that it matches the absorption profile of interest. In this way, if the optical path length (the distance between the source of light and the detector) and the absorption cross section are known, parameters such as the gas concentration can be calculated through the reduction in transmitted light (Lewander 2010).

2.3 Gas in Scattering Media Absorption Spectroscopy (GASMAS) technology

GASMAS is a relatively new aspect of gas spectroscopy which focuses on the absorption of light by gases enclosed in scattering media. The main concept behind this technology is based on the difference between the absorption of light by the free molecules of gases and molecules in liquids and solids. The free gas molecules, enclosed by scattering media, have unique sharp absorption imprints that are typically ten thousand times narrower than those of the surrounding media, making possible the detection of a very distinctive signal associated with the gas. When a tunable diode laser is scanned over the absorption imprint of a gas, an absorption signal of the order of 1×10^{-4} can be detected despite the heavy light absorption and scattering made by the surrounding bulk medium (Lewander 2010; Huang et al. 2015). The image below (figure 4) illustrates the concept behind this technology. There, three graphs that explains what happens when light passes through a porous medium are presented: the graph on top shows the intensity of light before this is injected into the sample, the one to the left shows the absorption of light (which is slowly varying) by the material surrounding the cavities and the last graph to the right shows the absorption dip created when light encounters a gas filled cavity in its path inside the sample.

In order to determine the concentration of a gas, the optical path length has to be first calculated. In the case of non-scattering medium, the optical path length is known, and it is the distance between the laser and the detector. In scattering media, photons travel through unknown gas distances due to the multiple scattering to which they are subjected. In this case an equivalent

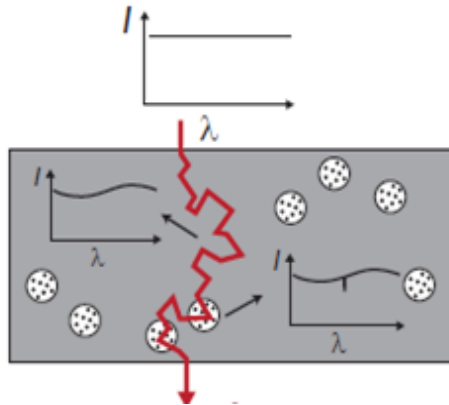


Fig. 4 Light absorption through a porous medium (Lewander 2010)

mean path length can be determined by measuring the distance that the photons have to cover through a reference gas, commonly ambient air, to be subjected to an absorption that is equivalent to the one experienced when traveling through the sample. However, conditions such as temperature, pressure and humidity, should be the same in the sample as in the reference ambient air for the equivalent path length to be the real distance the light has traveled in the sample (Persson et al. 2007; Lewander 2010). Usually, an absorption line that is close to the one of the gas in the sample is selected from the reference gas as it is assumed that similar wavelength might experience the same attenuation and scattering.

In this work the term absorption path length (APL) will be adopted instead of the term optical path length. This is because, here, the interest lies only on the distance travelled by light when going through the absorbing gas, the absorption by tissues and blood is ignored, opposite to the case where the term optical path length is used.

2.3.1 GASMAS biological applications

GASMAS technology can have a wide range of applications which includes analyzing gases inside sealed packages, gas bubbles in liquids, and gases enclosed by living tissues. This last case is of interest for this work as the focus here is on analyzing the oxygen concentration inside the sinuses.

Living tissues are relatively translucent to light in the optical window of 700-1100 nm, known as the tissue optical window (see figure 5), due to low light attenuation by tissue and by the different components of the blood (Blázquez-Castro 2019). The main absorbers in blood are oxygenated hemoglobin HbO_2 and deoxygenated hemoglobin Hb , which manifest high absorption for wavelengths under 700 nm. Water is another molecule that is abundant in tissues and manifests high absorption for wavelengths above 1100 nm (see figure 5) (Blázquez-Castro 2019).

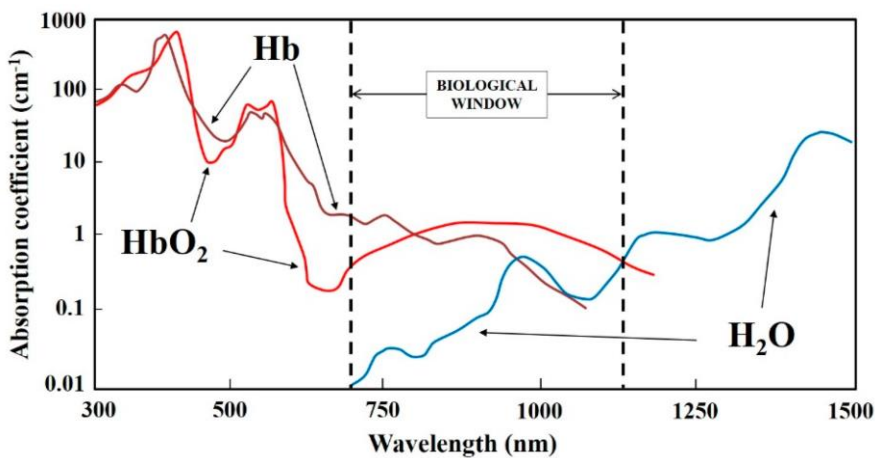


Fig. 5 Absorption of light by Hb , HbO_2 and H_2O . The tissue optical window can also be observed from the picture (Blázquez-Castro 2019).

As mentioned before, GASMAS is based on the strong spectroscopic contrast between the extremely sharp spectral features of free gases and those of solid materials. When considering the analysis of gases enclosed by living tissues, the difference between the sharp absorption fingerprints of the gases (O_2 and H_2O), and the slowly varying absorption fingerprints of the main blood components absorbers and lipids, can be clearly seen from figure 6.

The reference gas that is usually used when investigating cavities in the human body is water vapor. Its concentration inside the sinuses is known as it depends on the temperature and the relative humidity. The sinuses are

sparingly ventilated cavities with a temperature close to 32 °C (Evangelia et al. 2009; Zang et al. 2012), and they contain liquid water which leads to 98% relative humidity (Evangelia et al. 2009). From these parameters, the water vapor concentration is calculated to circa 4.6% or 45.9 ppm.

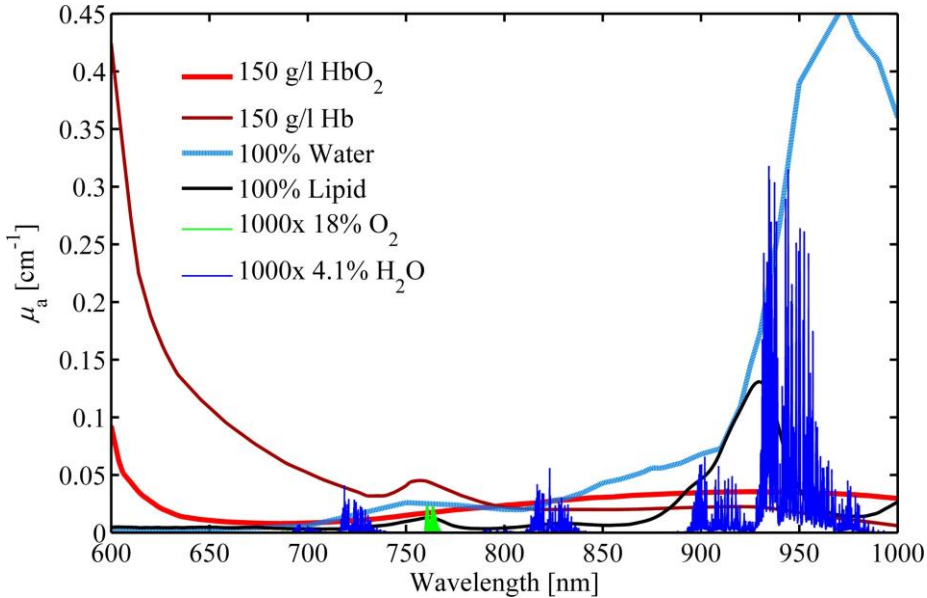


Fig. 6 Contrast between the sharp absorption lines of gases and the slowly varying absorption lines of the main absorbers present in blood (GPX Medical AB).

When having this information, the APL (which gives information about the sinus size) can be calculated as the relation between the height of the absorption curve and the concentration of water vapor, as will be explained later.

The oxygen concentration in the sinuses is generally around 16.3% (Aust and Dretner 1974), but a more precise estimation for each subject is needed. In this project, one absorption peak for O₂, at 764 nm, and one for H₂O at 820 nm were selected. These peaks can be seen in figure 7 and are the highest ones.

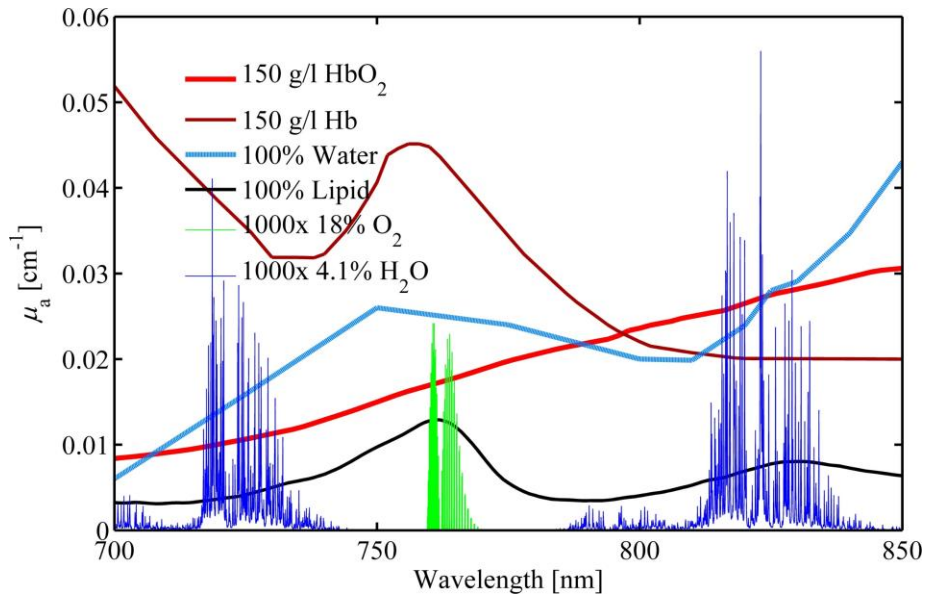


Fig. 7 This image contains the absorption profile of different elements. Here we are interested in the peaks selected for measuring the absorption of light by O₂ and H₂O, which are the highest ones for each element. (GPX Medical AB)

3 Method

This chapter is divided into three sections. In the first section there is a short description of the technical instruments used in the study. Here the probes used in this study are presented together with the probe geometries adopted for the different measurements' setups. The second section contains information about the pilot study which was performed to develop a clinical protocol for scientific studies. This protocol focuses mainly on the exposure time and the measurement geometry. Finally, the third section includes the study protocol and its setup. In this last part, the main protocol for the stability measurements under one-day, one-week and one-month is presented together with the method used to analyze the data.

3.1 Technical instruments

The instruments used in this study were:

- GPX Medical research device for GASMAS measurements (see figure 8)
- Fiber probes with two different geometries (see figure 9)
- A 10x10 mm detector probe (see figure 9b)
- A computer interface designed by GPX Medical to process the signals and to steer the laser system

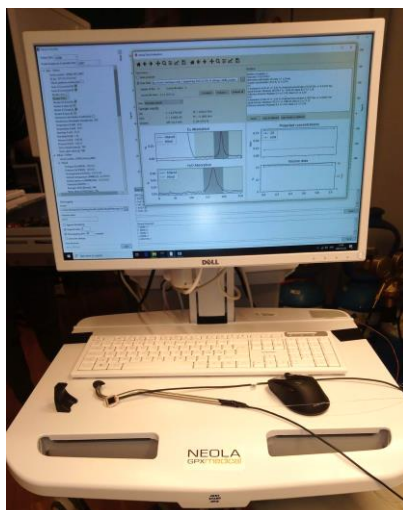


Fig. 8 Research device for GASMAS measurements developed by GPX Medical.



Fig. 9 Fiber probes. Figure 9a contains the probe that was used for measurements inside the mouth. Figure 9b, instead, contains the probe that was used for measurements outside the mouth. This probe contains the fiber on the top part and the detector on the bottom part. See figure 11 to better understand how the two probes were used for the measurements.

The laser system is designed in a way so that two lasers can be used almost simultaneously through time-multiplexing, to measure the absorption by molecular oxygen (O_2) and by water vapor (H_2O). The laser used for oxygen is calibrated at a wavelength of 764 nm. The laser for water vapor measurement, instead, is set to a wavelength of 820 nm. The desired wavelengths are obtained through temperature and current ramping. In this system a dual-wavelength setup is used, where each laser is active for 3.58

ms. For each O₂ measurement, a H₂O measurement is taken for reference. Thus, if the system takes a measurement over 1s, a total of 280 ramps are obtained ($3.58\text{ms} \times 280 = 1\text{s}$), 140 for oxygen and 140 for water vapor. The result is two signals, each of them is the average of 140 samples. The parameter that was investigated for the lasers was the number of ramps (measurements) to be averaged for each sample. This will be described in more detail in the next section.

In this study three probe geometries were determined, since three distinct measurement configurations were adopted. The first and the second measurement configuration consisted in placing the fiber probe in figure 9a inside the mouth and the detector under the eye. The third measurement configuration, instead, consisted in placing the probe in figure 9b so that the source of light is just under the middle of the eye and the detector under the cheekbone in line with the laser (see figure 11) . More details about the measurement protocol will be given in the next section.

The detector used in this study is a silicon type photodiode with a 10x10mm size.

3.2 Pilot Study

The first part of this work consisted in performing a pilot study to determine the probe/detector positions to be investigated in the next part of the work, the number of samples to average for each measurement and the number of measurements for each probe position. The probe/detector positions were determined by first analyzing a 3-D model of the sinuses, to gain better understanding about their morphology and position, and then by evaluating the O₂ signal strength in different positions around the maxillary sinuses of different volunteers, to determine the positions with stronger absorption signals. The signal strength was evaluated through the projected concentration, which is the height of the absorption signal shown in figure 10. This is a special measurement unit developed for measurements inside human cavities, and if divided by the percent of oxygen present in the measured cavity, it will give information about the size of the hollow.

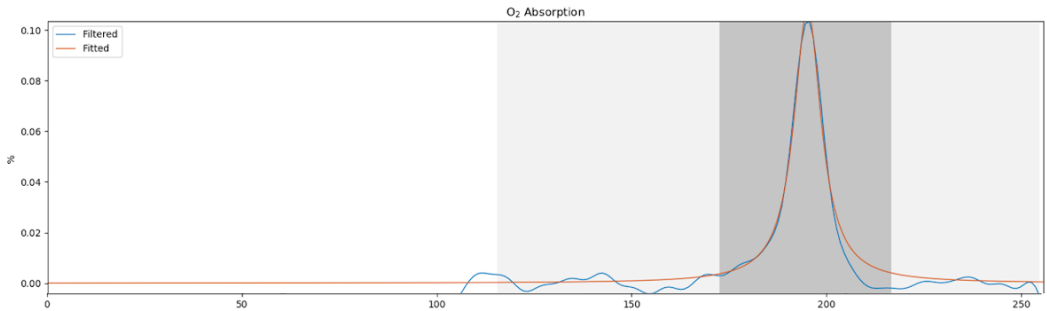


Fig. 10 Absorption signal for O₂

The projected concentration for water vapor (PC_{H₂O}) is also important for calculating the absorption path length (APL):

$$APL = PC_{H_2O} / \%H_2O$$

Finally, three measurement geometries were chosen.

In order to determine the number of samples to take for each measurement position and the updating time (number of ramps to average) of the laser signal, some preliminary measurements on the standard deviation of the projected concentration for O₂ were performed. At first, an updating time of 10s (average 1400 ramps for each laser) was chosen and, initially, 30 samples were taken for each measurement position. Afterwards, the same updating time was kept but 10 samples per measurement position were taken instead, because the whole measurement session became unnecessarily long (300s) and impractical for clinical measurements, where the time is often limited. However, in this last case as only a few samples were obtained per measurement, the standard deviation, in the analysis that followed, was not fairly represented. Thus, in order to determine the updating time of the laser and the number of samples, a longer measurement over five minutes, was taken with a small updating time of 0.5s for each sample. Then, the samples were bound by a script two by two to obtain a new updating time of 1s, four by four for an updating time of 2s and eight by eight for an updating time of 4s. Finally, the intervals of confidence for different updating times and different numbers of samples were calculated to compare the results and

select the optimal parameters. After determining the relevant parameters, the study protocol, that will be used in the next section, was designed.

3.3 Preclinical Study

This study consisted of collecting data on the instrument, and the sinuses size and oxygen concentration, by taking measurements on five volunteers, under a total period of one-month. The measurements were performed at different intervals of time:

- Four times in one-day, with two hours interval
- Once a day for five consecutive days
- Once a week for four weeks

The five volunteers participate in all sessions.

In each measurement session six measurements were taken, three for each sinus. The three measurement geometries are described in the pilot study (section 4.1). Each measurement is taken under a period of one minute, and the updating time of the laser is 2s as described in section 4.1.

The data obtained from the different volunteers is analyzed in order to determine the intra- and intersubject variability under the three periods of time, for both APL and oxygen concentration. The mean value and the standard error of the measurements performed under the different periods of time are plotted for each volunteer's right and left sinus and compared. Furthermore, the standard deviation of all O₂ and APL measurements taken under the three different periods are plotted to determine the instrument stability in time. Finally, a hypothesis test is also performed to determine if the APL measurements performed under the different periods of time, for each volunteer's right and left sinus, come from the same population. Our null hypothesis is that the measurements on the same subject's right/left sinus come from the same population and should not change in time, and this is verified with the ANOVA test.

4 Results and discussion

This section contains the results and the discussion of the pilot study and the preclinical study, together with the challenges encountered during this project.

4.1 Pilot Study

In this part, the results from the pilot study are presented together with a short discussion. The aim of the pilot study was to determine the updating time of the laser, the number of samples needed for each measurement, the consequent length of each measurement and the probe fiber-geometries.

The measurement geometries were determined qualitatively, by examining a 3-D model, and quantitatively by observing the change in the strength of the signal when probing in different positions.

Three detection geometries were chosen, as can be seen from figure 11:

- Palate - cheekbone, position 1: here the fiber is placed inside the mouth, in contact with the palate roof, close to the sinus under examination, and the detector is placed on the cheekbone, under the eye, close to the nose.
- Palate - cheekbone, position 2: here the fiber is in the same position as above, but the detector is moved circa 2 cm horizontally to be under the middle of the eye.

- Cheekbone - cheekbone, position 3: in this last position the fiber is placed on the cheekbone just under the middle of the eye and the detector is placed just under the cheekbone.

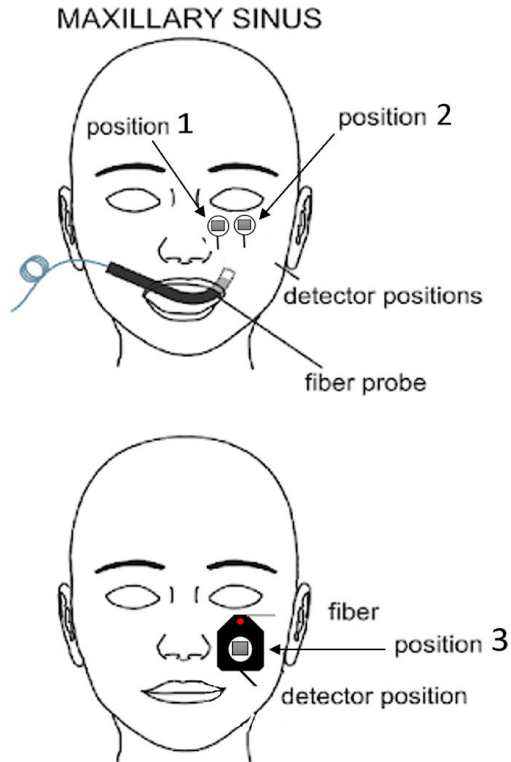


Fig. 11 Different probe/detector geometries. The picture on the top shows the two measurement configurations for the case when the fiber probe is placed inside the mouth. The picture below, instead, shows measurement configuration for the other case where the fiber is placed on the cheekbone under the middle of the eye (red light source) and the detector just under the cheekbone. This image was taken from (Lewander 2010) and modified with permission.

Regarding the measurement from inside the mouth, the volunteers are instructed to first insert the probe with the upper part (where the fiber emerges) in parallel to the palate, until it reaches the depth of the last molar,

and then to turn it circa 35 degrees towards the left or the right depending on the sinus under investigation.

The other parameters under investigation were determined by a quantitative analysis of data collected on three different volunteers. Here the interval of confidence was calculated for the projected concentration of O₂ taking an increasing number of samples and increasing updating time. Figure 12 shows the interval of confidence (calculated using two standard deviations) for the average projected concentration of oxygen, in %m, for different updating times and different number of samples in the same person. The samples were bound by a script two by two to obtain a new updating time of 1s, four by four for an updating time of 2s and eight by eight for an updating time of 4s as shown in figure 12. Here, we can see that the interval of confidence, for the different updating times, improves significantly until the measurement time reaches one minute. One minute is reached after 120 samples for 0.5s updating time, 60 samples for 1s updating time, 30 samples for 2s updating time and 15 samples for 4s updating time. After one minute, no appreciable development is observed. Furthermore, from figure 12 we can also see that the optimal updating time is either 1s or 2s which implies a number of samples of either 60 or 30.

The same procedure of binding data was followed for the data obtained from few other volunteers. The data from the other volunteers display a similar pattern to that observed for the first subject (see figure 13).

For volunteer 3 we did not consider the 0.5s updating time as it generally presents a high standard deviation which is not acceptable for our measurements. The 4s updating time was not considered either, as it did not necessarily give better results and the standard deviation was under-represented as we would only have 15 samples.

The data from volunteer 3 shows that 2s updating time is better than 1s as the interval of confidence is significantly smaller in the second case. This was a different result from the one obtained before, since the earlier results showed that 1s updating time is as good as 2s updating time under one minute of time.

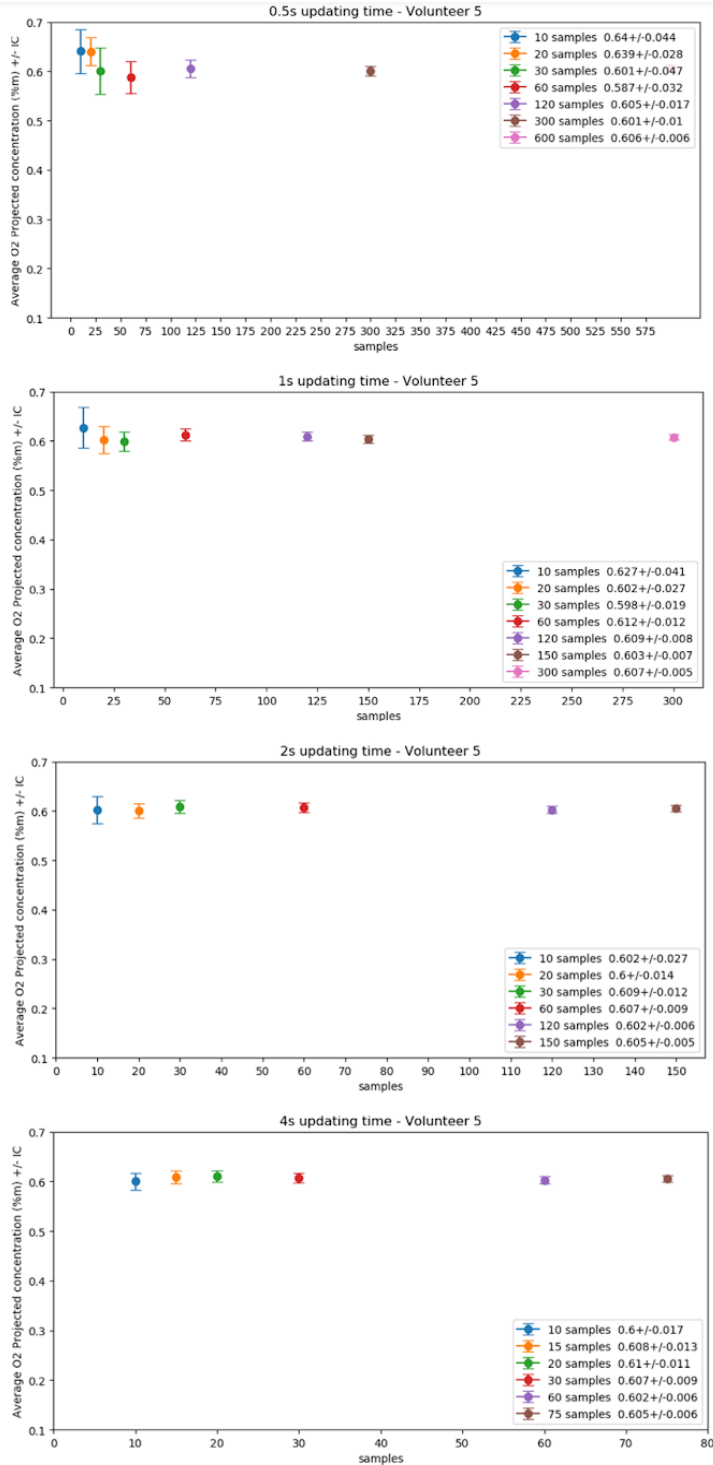


Fig 12. Average projected concentration (%m) and its interval of confidence (calculated considering two standard deviations) for a growing number of samples and different updating times. Data from volunteer 5.

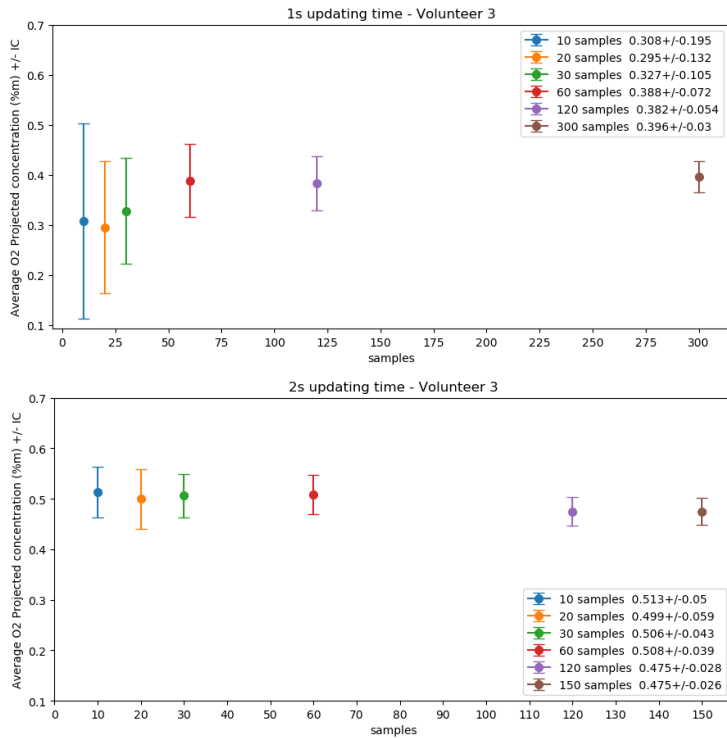


Fig. 13 Average projected concentration (%m) and its interval of confidence (calculated considering two standard deviations) for a growing number of samples and different updating times. Data from volunteer 3.

The plots for volunteer 4, presented in figure 14, confirms this last result, even if the difference is very small. Once again, 30 samples taken under one minute of time seems to be the best choice.

The results show that the best updating time is 2s and the optimal number of samples is 30. Thus, in the rest of the study each measurement will be carried under one minute with an updating time of 2s for each sample. One minute is a reasonable amount of time for clinical measurements.

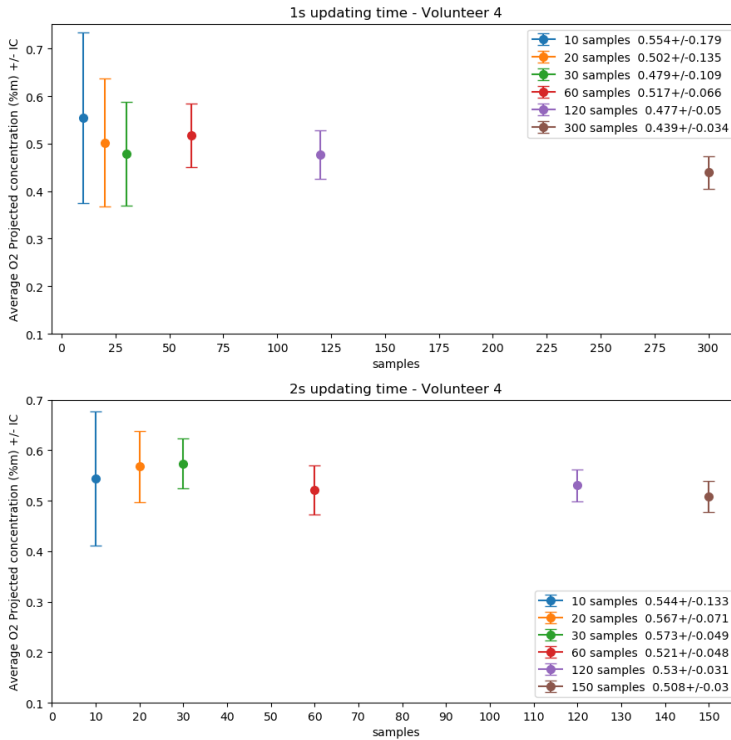


Fig. 14 Average projected concentration (%m) and its interval of confidence (calculated considering two standard deviations) for a growing number of samples and different updating times. Data from volunteer 4.

4.2 Preclinical Study

This section contains the analysis of the O₂ and H₂O transmission and absorption signals, which are shortly discussed and used to determine the best measurement position. It also contains the APL and O₂ concentration measurements results, obtained from the preclinical study, and the associated discussion. In this chapter the data from each volunteer is evaluated to analyze the intra subject variability followed by an analysis of the inter subject variability, where data from the different subjects is compared.

Five volunteers took part in this study and measurements on each volunteer's left and right sinus were taken under a period of one-day, five consecutive days and four weeks. This was done to later analyze the stability/variability of these measurements under the different periods of time. Each sinus was measured under three different probe-detector configurations in each measurement session (as described in section 4.1), to determine the configuration that gives the strongest absorption signal. These three configurations are named position 1, position 2 and position 3. Here, only data belonging to the position with the strongest signal is analyzed in detail for each volunteer.

Subsection 4.2.1 contains a short analysis of the oxygen transmission and absorption signal, and a description of the method used to choose the strongest signal for the different volunteers. Subsection 4.2.2 and 4.2.3 contain an analysis of the absorption path length and the O₂ concentration, respectively. In these two sections the intra- and intersubject stabilities are studied for the position with the strongest signal. Furthermore, the variance of the signals is analyzed to determine the stability of the instrument. Finally, some of the challenges encountered during this master thesis are presented in subsection 4.2.4.

4.2.1 O₂ and H₂O transmission and absorption signals for the different measurement positions

The O₂ and H₂O absorption and transmission signal for position 1, 2 and 3, for each volunteer, are shown in figure 15 and 16, respectively. Here all measurements periods are considered together. The plots show differences between the different positions, between the right and left side for the same subject and between the different subjects for both transmission and absorption of O₂ and H₂O.

The plots reveal that position 3 presents the highest amount of transmitted light in all cases, while position 1 shows the highest amount of absorbed light for all cases of O₂ and H₂O, except for the left sinus of volunteer 4,

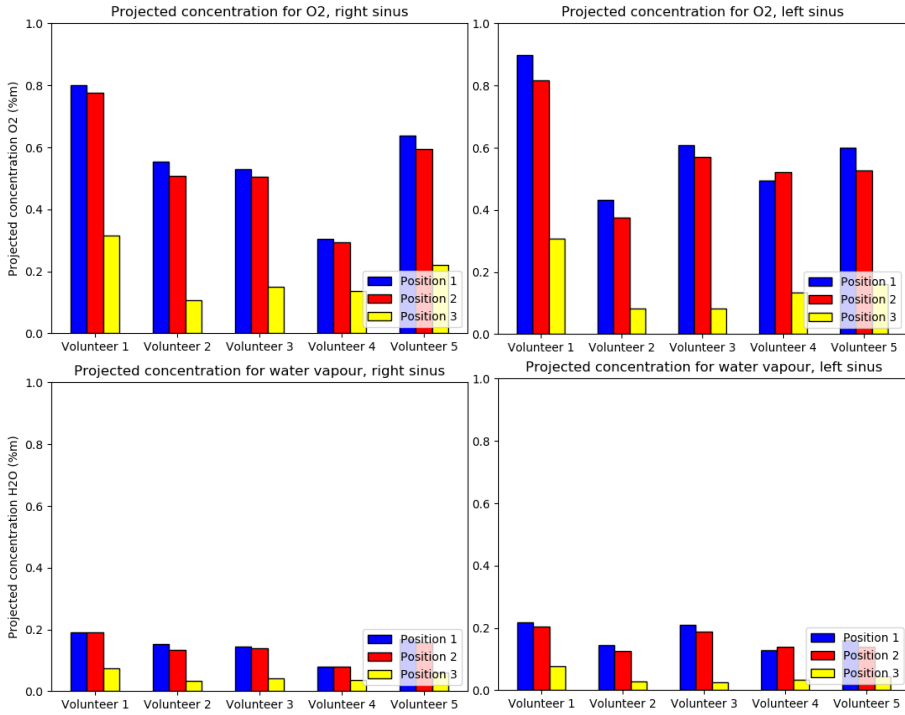


Fig. 15 Absorption signal for O₂ and water vapor.

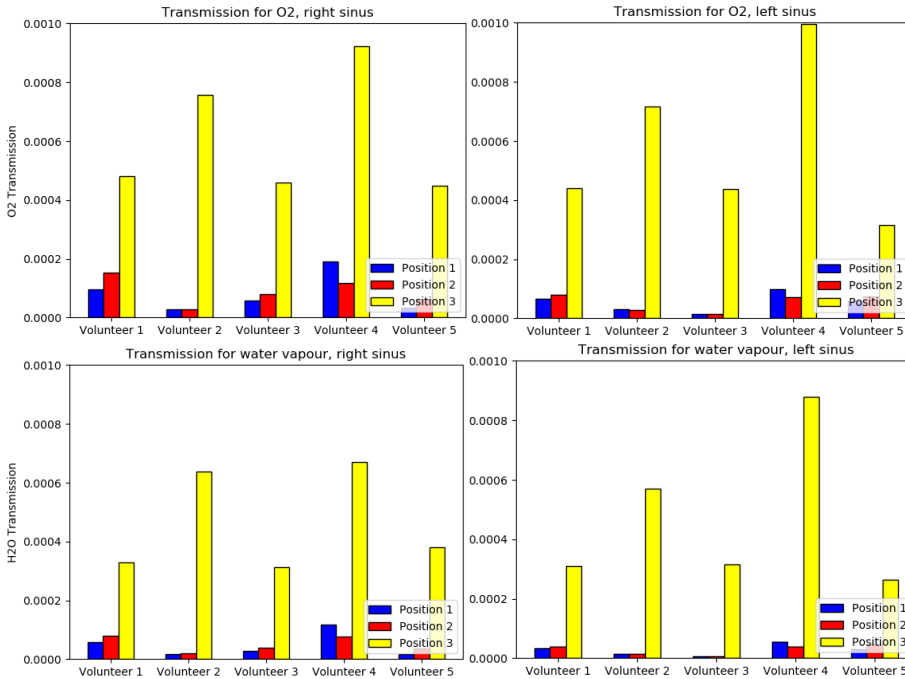


Fig. 16 Transmission for O₂ and water vapor.

which exhibits higher absorption for position 2. The high transmission / low absorption presented by the measurements on position 3, where the detector and the fiber probe are the closest, can be explained by the fact that, probably, most of the light did not pass throughout the sinuses, but went around them without encountering the gas in the cavities.

Considering the O₂ absorption signal, we can see from the images above that the differences between position 1 and 2 are not remarkable. However, position 1 exhibits a slightly stronger signal for all cases except one. Thus, the data from the first position will be examined for all cases except for the left sinus of volunteer 4, where, instead, data from the second position will be analyzed.

The reason why position 1 and 2 give a stronger signal, might be connected to the fact that by probing the sinuses from inside the mouth, we have a higher chance to reach the gas inside these cavities due to their shape in the side close to the nose, where a large sinus area is exposed (see figure 2). When measuring from position 3, it can happen that the light does not pass through the cavities, as mentioned before, but goes around them; due to the morphology of the sinuses there is less area to probe when adopting the cheekbone - cheekbone geometry. This can be further complicated by the fact that sinus size varies in different subjects making them, thus, more difficult to probe with this geometry.

From the plots, we can further observe that the projected concentration for water vapor is significantly smaller than that for oxygen. This is because we have higher concentration of oxygen compared to water vapor in our sinuses. In fact, assuming a temperature around 32 °C and a relative humidity of 98% in the sinuses we obtain that the water vapor concentration is around 4.6% compared to circa 20% for oxygen.

The differences between the probing positions, between the right and left side of each subject and the differences between the subjects, which can be seen from the above plots, are reflected in the measurements presented in the next sections.

4.2.2 Absorption path length (APL)

The data presented in the bar charts in figure 17 provides information about the average size of the right and the left sinus together with the standard error (SE), for each volunteer under a period of one-day, one-month and one-week. Here, the data from each volunteer will, first be examined individually then compared with data from other volunteers for a more general.

Volunteer 1

The APL stability measurements for this subject's right/left sinus have respective values of 36/50 mm with 0.8/2 mm SE for one-day stability, 45/47 mm with 3.5/3.9 mm SE for one-week stability, and 43/46 mm with 2.8/3.1 mm SE for one-month stability. The data for this subject suggests that the left sinus is slightly larger than the right one.

Volunteer 2

The second subject's APL data for the right/left sinus have respective values of 38/39 mm with 5.9/9.7 mm SE for one-day stability, 30/26 mm with 3.2/3.4 mm SE for one-week stability, and 34/33 mm with 3.8/3.2 mm SE for one-month stability. Most of the data gathered from this subject, considering all three positions, imply that this volunteer's right sinus is slightly larger than the left one. The data for the one-day stability measurements suggest a larger left sinus, however, this difference is very small and the fact the left sinus value is accompanied by larger standard error allows us to confirm the above statement of a slightly larger right sinus. It was generally difficult to obtain good signals from this subject's sinuses. This could be partly attributed to the fact that this subject was not as familiar with the probes positioning as the other subjects.

Volunteer 3

This volunteer's APL stability measurements for the right/left sinus have respective values of 33/47 mm with 3.8/9.3 mm SE for one-day stability, 31/42 mm with 3.1/6.3 mm SE for one-week stability, and 32/47 mm with 3.9/7.4 mm SE for one-month stability. This subject also presents a

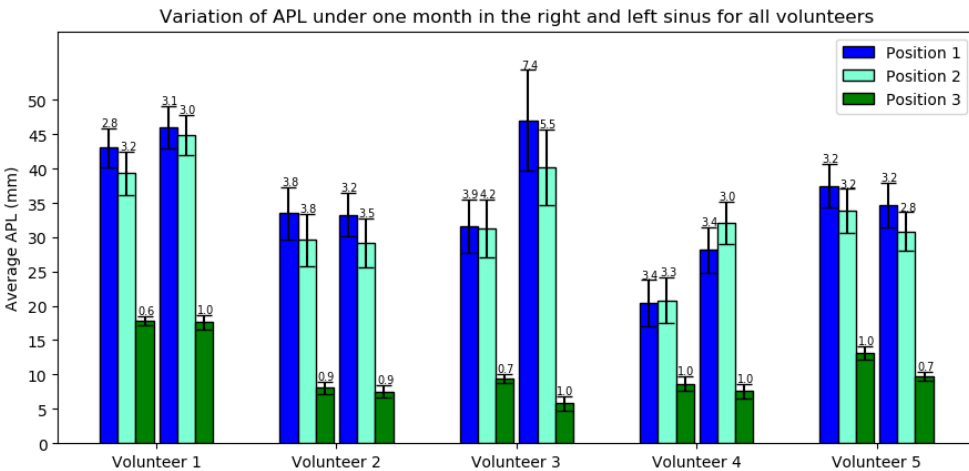
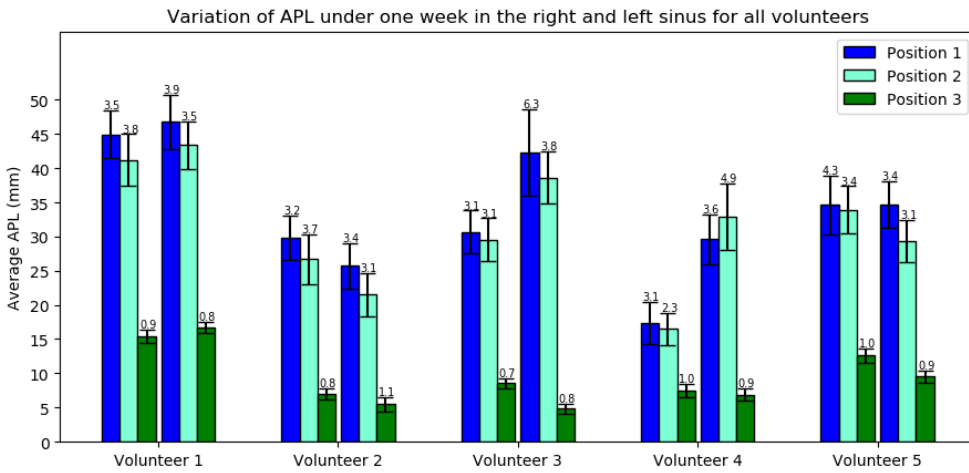
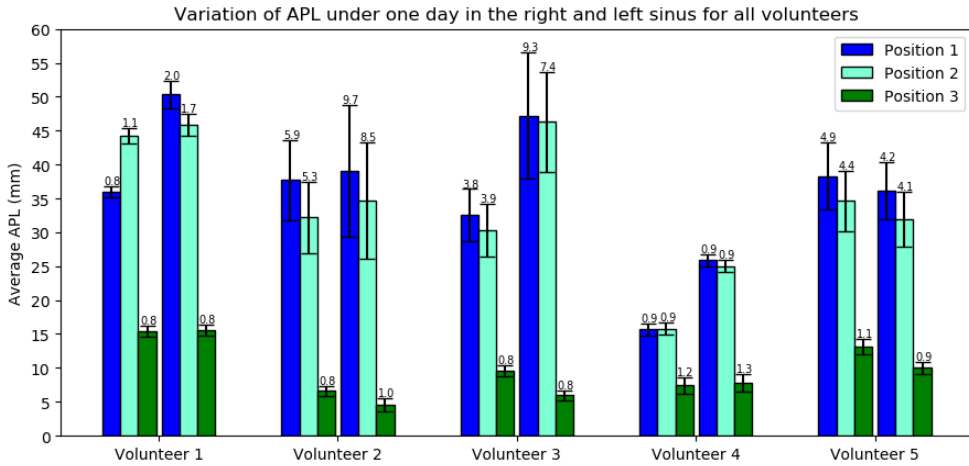


Fig.17 APL stability measurements for the right (first three values) and left sinus (last three) of each volunteer, together with the standard error.

difference in size between the right and left sinus as the left one seems to be larger. It was particularly difficult to take good quality measurements on this subject's left side and this is confirmed by the higher standard error associated with the left side compared to the right one.

Volunteer 4

The fourth volunteer's APL stability measurements for the right/left sinus have values of 16/25 mm with 0.9/0.9 mm SE for one-day stability, 17/33 mm with 3/4.8 mm SE for one-week stability, and 20/32 mm with 3.4/3 mm SE for one-month stability, respectively. Even this volunteer has a larger left sinus. However, contrary to the previous subject, whose left sinus was difficult to measure, here, it was slightly more difficult to collect data on the right sinus. This could be attributed to the fact that this volunteer has a small right sinus compared to the other volunteers, which makes it more difficult to probe.

Volunteer 5

The last subject's APL stability measurements for the right/left sinus present values of 38/36 mm with 5/4.2 mm SE for one-day stability, 35/35 mm with 4.3/3.4 mm SE for one-week stability, and 37/35 mm with 3.2/3.2 mm SE for one-month stability, respectively. Considering even data from other positions, for this last volunteer, the right sinus is slightly larger than the left one; however, the difference is very small.

Volunteer 1 presents larger right and left sinuses together with volunteer 2 who has larger left sinus and volunteer 5 with larger right sinus, compared to the other subjects. Volunteer 4 has the smallest right and left sinuses except for one-week stability measurements where volunteer 2 has smaller left sinus. The differences between the right and left side are substantial for subject 3 and 4 where this difference is larger than 10 mm in all cases except one. For the other volunteers, instead, the differences are only a few mm; the largest difference is about 4 mm for these other subjects.

Considering all the measurements together, the standard error varied in the range 0.8-9.7 mm. However, its distribution was different for the different

subjects with most values lying under 4 mm, which can be considered a good result.

In the study performed by Persson L. et al. in 2007 it was found that the maxillary sinuses size of 10 healthy volunteers varied between 10 mm and 40 mm, with a 10% average standard deviation, when the palate-cheekbone geometry was adopted (Persson et al. 2007). This result is close to the result obtained from this study where the sinuses sizes vary in the interval 16-50 mm. However, in the mentioned study, a wavelength of 935 nm was used for water vapor compared to the 820 nm wavelength used here. Additionally, the measurement system set-up and some of the assumptions were also different.

Consistent asymmetries between the right and left side of the different volunteers were observed also in the study performed by Persson L. et al. and in the study performed by Huang J. et al, in 2015 (Huang et al. 2015). However, in this last study, only the frontal sinuses were analyzed. The results obtained from this study and from the above-mentioned studies are not precise but only give indication about the expected sizes of typical healthy sinuses, thus variations are expected.

If we observe the one-day stability measurements for volunteer 1 and 4, we can see from figure 17 that their standard error is smaller compared to that of the other subjects, and it is also smaller than the standard error found in other periods, for the same subjects. This is due to the fact that the in last two days of measurements we changed fiber for the measurements on position 1 and 2, realizing, thus, that the previous fiber was significantly damaged and contributed to a larger variability. The same was observed for the measurements taken for the other volunteers under the last two days. However these last values are not visible in the graphs because these other subjects did their one-day stability measurements one-day before we changed the fiber, and the measurements taken with the new fiber are combined with the other measurements for the one-week and one-month stability measurements. From the graphs, we can also see that position 3, for which we used a different fiber from the beginning, always has a smaller standard error compared to the other positions. At the beginning we

suspected that, even if position 3 presented a weaker absorption signal, it was better suited for the sinus measurements because it always exhibited lower standard deviation. This was, however, disproved when we changed fiber for position 1 and 2, because after this change, the measurements, in addition to a stronger absorption signal, also exhibited a considerably lower standard deviation and standard error. The standard error size can be also attributed to the fact that it was not possible to take measurements on the exact same position every time. Furthermore, it was also difficult for the volunteers to keep completely still during the measurements.

The image below shows the standard deviation for the measurements performed on all volunteers under the three periods of time.

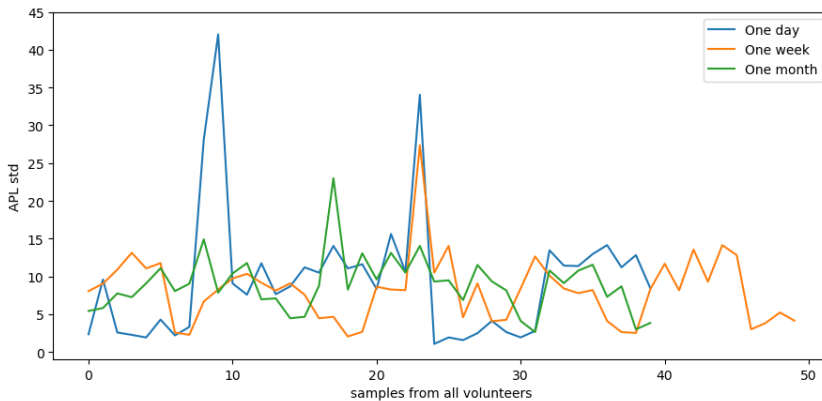


Fig. 18 APL standard deviation for all volunteers' measurements, position 1.

From the graph, it is clear that, except for a few outliers, the measurements performed under the three periods of time have a similar standard error, which means that the instrument performance is more or less stable in time. The outliers are attributed to the subjects on whom it was difficult to perform good quality measurements.

Anova test

In order to determine if the APL values for each volunteer were stable between the one-day, one-week and one-month measurements, the statistical test ANOVA test is used. The aim of this test is to analyze the differences between the means of the measurements performed under the

three periods of time, for each volunteer, and determine if they are equal. The null hypothesis, H_0 , for this test is that the means of the three groups are the same while the alternate hypothesis is that at least one of the means is different.

Here, for each volunteer, we assume the following:

- Each sample is taken from a normally distributed population
- The samples are independent from each other
- The variance in the different groups is the same

The significance level used here is $\alpha = 0.05$. This value indicates a 5% risk of concluding that there is a difference between the means when there is not (rejecting falsely the null hypothesis). The p-value, instead, is the area under the right side of the F statistic obtained from the ANOVA table. If this value is larger than α then we do not have enough evidence to reject the null hypothesis and thus we consider the different means to be equal. One other way to check if the obtained results are not significant enough to reject the null hypothesis is to compare the F-value (defined as between group variability/ within group variability) with F-critical found in the F table for $\alpha = 0.05$. If the F-value is larger than F-critical, we reject H_0 , but only if the p-value is smaller than α . The F-value should always be used together with the p-value to decide whether to reject or not the null hypothesis.

The table below shows the results of the ANOVA test performed on the means of the values collected under the three periods of time, for each volunteer's right and left sinus (where R=right and L=left).

From table 1 we can conclude that the one-day, one-week and one-month measurements come from the same population for volunteers 1, 3 and 5 for both sides, which means that the measurements were stable under the three periods of time. For volunteer 4 the means are from the same population only for the right sinus while for subject 2 the means are different for both sides, implying instability in the measurements. Rejecting the null hypothesis means that at least one of the means comes from a different population. This result indicates instability in the measurements of some volunteers. This instability could depend on the instrument, the way the volunteers held the probes, the sinus morphology, the quality of the fiber or

the fact that sometimes the fiber slipped slightly inside the probe during the measurements. Furthermore, the fact that the H_0 was rejected only for volunteers whose sinuses were difficult to probe might suggest that the instability in the measurements is subject dependent rather than instrument dependent.

$\alpha = 0.05$	Volunteer1		Volunteer2		Volunteer3		Volunteer4		Volunteer5	
sinus	R	L	R	L	R	L	R	L	R	L
p-value	0.06	0.68	0.40	0.22	0.92	0.85	0.56	0.20	0.87	0.98
F value	2.86	0.38	0.92	1.50	0.09	0.16	0.59	1.59	0.13	0.02
F critical	2.9957		2.9957		2.9957		2.9957		2.9957	
Accept H_0	✓	✓	✗	✗	✓	✓	✓	✗	✓	✓

Table 1 Results from ANOVA Test analysis

4.2.3 Oxygen concentration

This section presents and discusses the data in figure 19, for the one-day, one-week and one-month stability measurements for the oxygen concentration, for each volunteer's right and left sinus. Here, since fluctuations in oxygen concentration are small within the same sinus, across the different periods, for all subjects, the data will be described considering the one-day, one-week and one-month stability measurement periods together.

Volunteer 1

The O_2 concentration in the first volunteer's right and left sinus fluctuates in the range 19-20% with a standard error in the range 0.7-2.4%. No significant differences in O_2 concentration between the right and the left sinus have been observed for this individual.

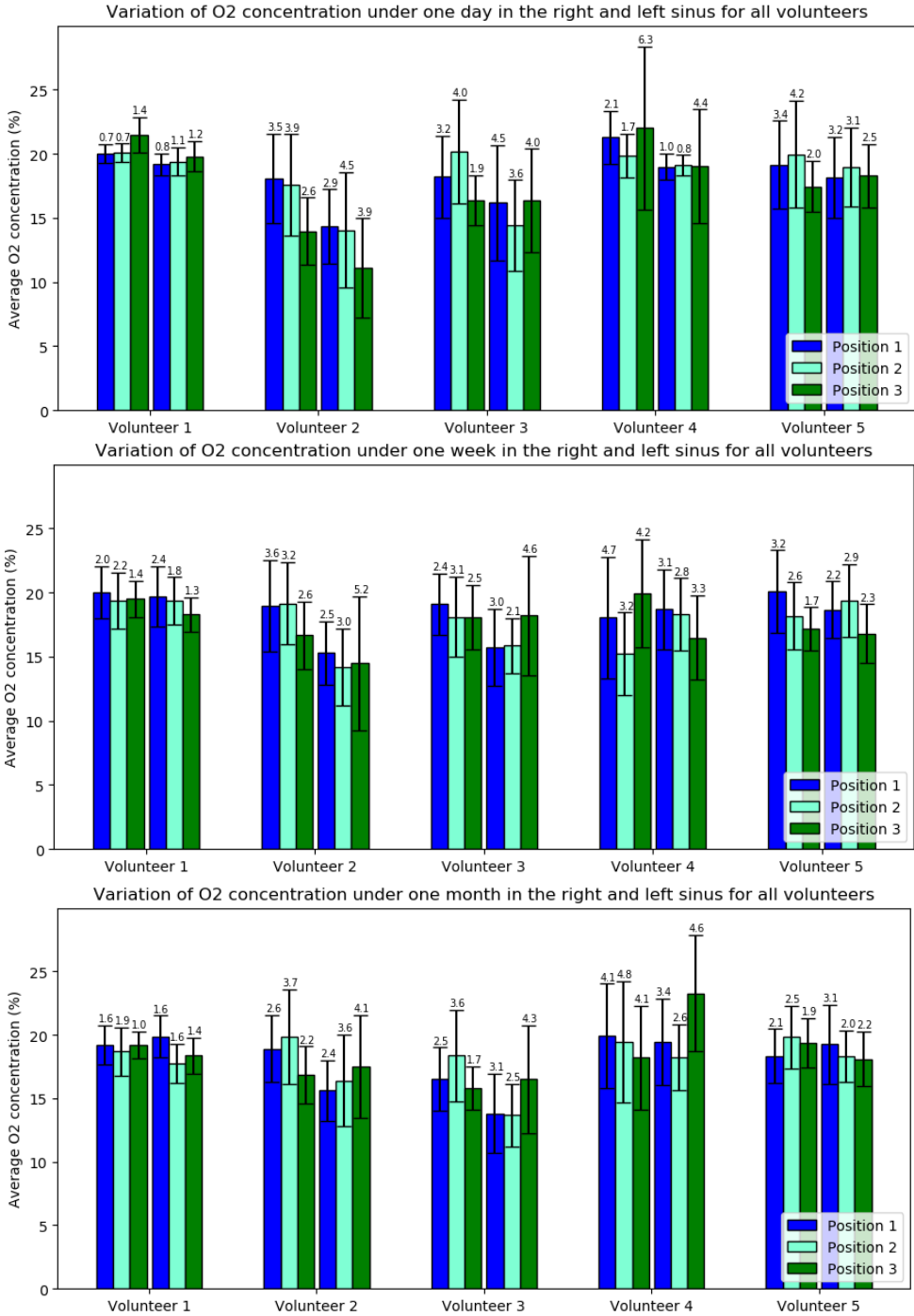


Fig.19 O2 concentration stability measurements for the right (first three values) and left sinus (last three) of each volunteer, together with the standard error.

Volunteer 2

For this volunteer, the O₂ concentration values are in the range 18-19 % with a standard error of 2.6-3.6% for the right sinus and 14-16% with a 2-3% standard error for the left sinus. Here, the right sinus seems to have higher oxygen concentration.

Volunteer 3

The third subject's O₂ concentration stability measurements show a variability in the interval 17-19% with a standard error in the interval 2.4-3.2% for the right sinus and 14-16% with a standard error in the range 3-4.5% for the left sinus. Even this subject presents a small difference between the two sides.

Volunteer 4

This volunteer exhibits O₂ concentration values in the span 18-21% with 2.1-4.7% standard error for the right side and 18-19% with 2.6-3.2 standard error for the left sinus. This subject presents no clear difference between the two sides.

Volunteer 5

The last subject's O₂ stability measurements stretch over a span of 18-20% with an error of 2.1-3.4 for the right sinus and 18-19% with an error of 2.1-3.2% for the left sinus. The difference between the two sides is neglectable also in this case.

The standard error for subjects 1 and 4 under one-day stability measurements are lower here too, because of the fiber change as described in section 4.2.1.

Volunteers 1, 4 and 5 present an O₂ concentration in the range 18-21% for both sinuses and no significant differences between the two sides. Both volunteers 2 and 3 exhibit a smaller O₂ concentration of 14-16% for the left sinus. The second volunteer's right side O₂ concentration is in the range 17-19% which is close to the 18-21% range, while the third volunteer's right-side value lies in the above range of 18-21%.

This is an encouraging result as the ranges described above are close to the value of 16.3%, which represents oxygen concentration in the sinuses with a patent ostium (Aust and Drettner 1974).

The standard error for all water vapor measurements, spans in the range 0.7-4.7% with most values under 3.5%. Even here, the standard error is affected by the small changes in position between the different sessions and the movements of the volunteers when holding the probes.

The standard deviations for all O₂ concentration measurements performed under one-day, one-week and one-month are presented in figure 20. The plot shows that the standard deviation values are generally stable under the different periods of time, suggesting a certain stability of the instrument.

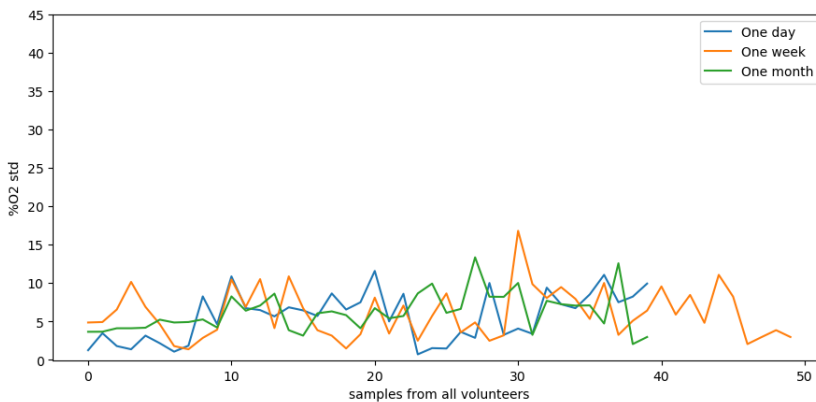


Fig. 20 Oxygen concentration standard deviation for all volunteers' measurements, position 1.

4.2.4 Challenges

During this project, several challenges emerged under the way. Some of the challenges are related to the measurement instruments and some are related to the measurements themselves.

The difficulties encountered with the measurement instrument include the challenges met with the water vapor laser system, which shut off in many occasions during the measurements, and the digital communication between the laser system and the motherboard which failed in several occasions. Additionally, the laser system was undergoing a slow degradation. Furthermore, the fiber used in the measurements inside the mouth also degraded but at a faster rate, however we were not fully aware of this fact. In fact, as explained previously, just in the last two days of measurements we changed this fiber and noticed a remarkably better result in the stability measurements. This fiber also glided out from the probe in multiple episodes, causing errors in the measurements. All these facts affected the measurements which had to be repeated on several occasions.

Some of the problems encountered with the measurements involve the measurements positions and the difficulties to measure on certain subjects. It was generally difficult to place the probes on the exact same positions every time. The volunteers were given instruction on how to place the probes, but this did not guarantee the exact same placement on each occasion, also because the volunteers had to move the probe to find a good signal each time. However, the palate - cheekbone transmission geometry (position 1 and 2 inside the mouth) provided reproducible signal and was not particularly sensitive to smaller variations in probes positioning. This is because of the large area of sinus exposed when measuring from inside the mouth. On the other side the cheekbone - cheekbone geometry (position 3 outside the mouth) presented lower tolerance to changes in probes positions and in most cases, it took longer time to find the right spots to probe. Furthermore, the volunteers were not completely still during the measurements, causing changes in probe positions. Considering the measurements on the different subjects, it was more difficult to obtain good data from volunteer 2, 3 and 4 compared to volunteer 1 and 5. Nevertheless this was true only for one of their sinuses except for volunteer 2 where both sinuses were particularly difficult to probe. These volunteers had a larger amount of rejected data and presented several outliers. The reason for this could be partly explained by the fact that they might have smaller right and/or left sinus, a fact that makes the probing of these cavities more

challenging, and this is also partly shown by their results of some of them.

5 Conclusions

This project is the first of its type, only few other studies were done in this area and they focused on different things. Here five volunteers were followed under a longer period to obtain more comprehensive data about the sinuses size, O₂ concentration and measurements stability. This is important for the development of the medical device that in the near future could support doctors in determining if a sinus inflammation is caused by virus or bacteria, leading to a reduction in the use of antibiotics and decrease in deaths associated with antimicrobial resistance in the future.

The analysis in section 4.2.1 showed that the best detector-fiber geometry for the measurements is, generally, the palate-cheekbone geometry, referred to as position 1. This first analysis led to focusing mainly on data from this geometry. Data from position 1 presented relatively low intra-subject variability. The APL measurements, for the sinuses belonging to volunteers 1, 3 and 5 and for the right sinus of volunteer 4 were stable across the periods of time that were under examination. In fact, the ANOVA test showed that the mean APL across the three periods of time comes from the same population for these volunteers. However, for the left sinus of volunteer 4 and both sinuses volunteer 2 the test showed instabilities in the measurements. These last volunteers are the same for whom it was difficult to obtain a good signal. This fact might suggest that the instabilities encountered during these measurements can be subject dependent. Differences between the right and the left sinus, within the same subject, were encountered in most cases as happened in other studies. The sinuses

average sizes ranged from 16 mm to 50 mm, with most values in the interval 30-47 mm, across the different subjects, revealing a certain inter-subject variability. The oxygen concentration values, for each subject, were stable across the different periods of time and in most cases did not differ significantly between the right and the left sinus. In most cases, the oxygen levels were stable even across different subjects with values in the range 18-20%. Only volunteers 2 and 3 had a different oxygen concentration compared to other subjects and these differences were only found in the left sinus, with values in the interval 14-16%. The analysis of the standard deviation of all APL and O₂ measurements showed that the instrument performance was approximately the same under one-day, one-week and one-month.

To sum up, the measurements across one-day, one-week and one-month presented a certain stability. The instability encountered for certain volunteers is suspected to be subject based rather than instrument based. A better stability level was observed for measurements on position 1 and 2, taken with a newer fiber, and for measurements on position 3 where a different fiber was used from the beginning. There, the standard deviation, and standard error were significantly lower than the general cases. However, the measurements on position 2 and 3 with the newer fiber were only performed under the last two days of the study, thus in order to obtain more accurate results, the measurements performed on these two positions should be repeated with a better fiber.

6 Bibliography

Alsaied, A.S. 2017. Paranasal Sinuses. In: *Paranasal Sinus Anatomy: What the Surgeon Needs to Know*.

Aust, R. and Drettner, B. 1974. Experimental studies of the gas exchange through the ostium of the maxillary sinus. *Upsala journal of medical sciences* 79(3), pp. 177–186.

Blázquez-Castro, A. 2019. Optical tweezers: phototoxicity and thermal stress in cells and biomolecules. *Micromachines* 10(8).

Evangelia, T., Vasileios, K., Richard, L., Gerhard, R. and Joerg, L. 2009. Temperature and humidity measurements in nasal cavity. In: *IEEE*, pp. 69–72.

Fatterpekar, G.M., Delman, B.N. and Som, P.M. 2008. Imaging the paranasal sinuses: where we are and where we are going. *Anatomical Record* 291(11), pp. 1564–1572.

Huang, J., Zhang, H., Li, T., Lin, H., Svanberg, K. and Svanberg, S. 2015. Assessment of human sinus cavity air volume using tunable diode laser spectroscopy, with application to sinusitis diagnostics. *Journal of biophotonics* 8(11–12), pp. 985–992.

Jankowski, R., Nguyen, D.T., Poussel, M., Chenuel, B., Gallet, P. and Rumeau, C. 2016. Sinusology. *European annals of otorhinolaryngology, head and neck diseases* 133(4), pp. 263–268.

Jørgensen, L.C., Friis Christensen, S., Cordoba Currea, G., Llor, C. and Bjerrum, L. 2013. Antibiotic prescribing in patients with acute rhinosinusitis is not in agreement with European recommendations. *Scandinavian journal of primary health care* 31(2), pp. 101–105.

Larsson, J., Leander, D., Lewander Xu, M., Fellman, V., Bood, J. and Krite

- Svanberg, E. 2019. Comparison of dermal vs internal light administration in human lungs using the TDLAS-GASMAS technique-Phantom studies. *Journal of biophotonics* 12(8), p. e201800350.
- Lewander, M. 2010. Laser Absorption Spectroscopy of Gas in Scattering Media. Doctoral dissertation. Division of Atomic Physics. Department of Physics. Faculty of Engineering, LTH Lund University.
- Morcom, S., Phillips, N., Pastuszek, A. and Timperley, D. 2016. Sinusitis. *Australian Family Physician* 45(6), pp. 374–377.
- Parson, W.W. 2015. *Modern Optical Spectroscopy*. 2nd ed. Berlin, Heidelberg: Springer Berlin Heidelberg.
- Persson, L., Andersson, M., Cassel-Engquist, M., Svanberg, K. and Svanberg, S. 2007. Gas monitoring in human sinuses using tunable diode laser spectroscopy. *Journal of Biomedical Optics* 12(5), p. 054001.
- Raut, A.A. and Jankharia, B. 2009. Paranasal sinuses in health and disease. In: Stucker, F. J., de Souza, C., Kenyon, G. S., Lian, T. S., Draf, W., and Schick, B. eds. *Rhinology and facial plastic surgery*. Berlin, Heidelberg: Springer Berlin Heidelberg, pp. 35–62.
- Rosenfeld, R.M. 2016. CLINICAL PRACTICE. acute sinusitis in adults. *The New England Journal of Medicine* 375(10), pp. 962–970.
- Zang, H., Liu, Y., Han, D., et al. 2012. Airflow and temperature distribution inside the maxillary sinus: a computational fluid dynamics simulation. *Acta Oto-Laryngologica* 132(6), pp. 637–644.
- Zinreich, S.J., Kennedy, D.W., Rosenbaum, A.E., Gayler, B.W., Kumar, A.J. and Stammberger, H. 1987. Paranasal sinuses: CT imaging requirements for endoscopic surgery. *Radiology* 163(3), pp. 769–775.